
Safety and Efficacy of ^{166}Ho Radioembolization in Hepatocellular Carcinoma: The HEPAR Primary Study

Margot T.M. Reinders¹, Karel J. van Erpecum², Maarten L.J. Smits¹, Arthur J.A.T. Braat¹, Joep de Bruijne², Rutger Bruijnen¹, Dave Sprengers³, Robert A. de Man³, Erik Vegt⁴, Jan N.M. IJzermans⁵, Adriaan Moelker⁴, and Marnix G.E.H. Lam¹

¹Department of Radiology and Nuclear Medicine, University Medical Centre, Utrecht University, Utrecht, The Netherlands;

²Department of Gastroenterology and Hepatology University Medical Centre, Utrecht University, Utrecht, The Netherlands;

³Department of Gastroenterology and Hepatology, Erasmus MC–University Medical Centre, Rotterdam, The Netherlands;

⁴Department of Radiology and Nuclear Medicine, Erasmus MC–University Medical Centre, Rotterdam, The Netherlands; and

⁵Department of Surgery, Erasmus MC–University Medical Centre, Rotterdam, The Netherlands

The safety and efficacy of ^{166}Ho radioembolization was first determined in the HEPAR and HEPAR II studies, which, however, excluded patients with hepatocellular carcinoma (HCC). The aim of this prospective clinical early phase II study was to establish the toxicity profile of ^{166}Ho radioembolization in patients with measurable, liver-dominant HCC; Barcelona clinic liver cancer stage B or C; a Child–Pugh score of no more than B7; and an Eastern Cooperative Oncology Group performance status of 0–1 without curative treatment options. **Methods:** The primary endpoint was a rate of unacceptable toxicity defined as grade 3 hyperbilirubinemia (Common Terminology Cancer Adverse Events, version 4.03) in combination with a low albumin or ascites level in the absence of disease progression or treatment-related serious adverse events. Secondary endpoints included overall toxicity, response, survival, change in α -fetoprotein, and quality of life. Thirty-one patients with Barcelona clinic liver cancer stage B (71%) or C (29%) HCC were included, mostly multifocal (87%) or bilobar (55%) disease. **Results:** Common grade 1 or 2 clinical toxicity included fatigue (71%), back pain (55%), ascites (32%), dyspnea (23%), nausea (23%), and abdominal pain (23%), with no more than 10% grade 3–5 toxicity. Grade 3 laboratory toxicity (>10%) included an aspartate transaminase and γ -glutamyltransferase increase (16%), hyperglycemia (19%), and lymphopenia (29%). Treatment-related unacceptable toxicity occurred in 3 of 31 patients. At 3 mo, 54% of target lesions showed a complete or partial response according to modified RECIST. Median overall survival was 14.9 mo (95% CI, 10.4–24.9 mo). No significant changes in quality of life or pain were observed. **Conclusion:** The safety of ^{166}Ho radioembolization was confirmed in HCC, with less than 10% unacceptable toxicity. Efficacy data support further evaluation.

Key Words: hepatocellular carcinoma; radioembolization; holmium; oncology; locoregional treatment

J Nucl Med 2022; 63:1891–1898

DOI: 10.2967/jnumed.122.263823

The treatment landscape for patients with hepatocellular carcinoma (HCC) consists of transplantation, resection, locoregional

treatment options (including ablation, transarterial chemoembolization, and radioembolization), and systemic treatment options (targeted therapy and immunotherapy) (1–3). Despite therapeutic advances, prognosis remains poor. Only a minority of patients is eligible for curative treatment (e.g., transplantation, resection, and in some cases ablation). ^{90}Y radioembolization is often used in selected patients with HCC without curative treatment options (4).

Microspheres loaded with ^{166}Ho have been commercially available since 2015 (QuiremScout and QuiremSpheres; Quirem Medical B.V.). ^{166}Ho is a high-energy β -emitting isotope with a maximum energy of 1.85 MeV (50.0%) and 1.77 MeV (48.7%), comparable to the 2.28 MeV for ^{90}Y but with a half-life of 26.8 h, which is approximately half that of ^{90}Y (i.e., 64 h). The main advantage over ^{90}Y is the abundance of γ -photons (81 keV, 6.7%) that can be used for SPECT/CT imaging (5). Furthermore, because the lanthanide ^{166}Ho has paramagnetic properties, MRI can also be used to image the distribution in the liver and quantify the absorbed dose in the tumors (6). These unique characteristics improve pre- and posttherapeutic imaging options, enabling dosimetry-based individualized treatment planning. The mean diameter of ^{166}Ho -microspheres is 30 μm , with a range of 15–60 μm , comparable to both types of ^{90}Y -microspheres. The density of ^{166}Ho -microspheres is 1.4 g/cm^3 , which is comparable to the density of resin ^{90}Y -microspheres but lower than glass ^{90}Y -microspheres.

The safety and efficacy of ^{166}Ho radioembolization was first determined in the HEPAR and HEPAR II studies in patients with liver metastases of different types of cancer origin, excluding HCC (7,8). The aim of this clinical early phase II study was to establish the safety and toxicity profile of ^{166}Ho radioembolization in patients with HCC.

MATERIALS AND METHODS

Study Population and Design

The HEPAR Primary study (NCT03379844) was a multicenter interventional, nonrandomized, noncomparative open-label early phase II study in patients with Barcelona clinic liver cancer (BCLC) stage B or C HCC, treated between January 28, 2018, and February 18, 2020. The study protocol was approved by the independent Medical Ethics Committee and was performed in accordance with good clinical practice and the declaration of Helsinki. All participants provided written informed consent.

The main inclusion and exclusion criteria were an age of at least 18 y with a life expectancy of at least 6 mo, a diagnosis of HCC according to

Received Jan. 15, 2022; revision accepted Apr. 18, 2022.

For correspondence, contact Margot T.M. Reinders (m.t.m.reinders@umcutrecht.nl); for reprint requests, contact Marnix G.E.H. Lam (m.lam@umcutrecht.nl).

Published online May 19, 2022.

COPYRIGHT © 2022 by the Society of Nuclear Medicine and Molecular Imaging.

the criteria of the American Association for the Study of Liver Disease (9), a measurable lesion based on RECIST (RECIST 1.1 and mRECIST), liver-dominant disease (a maximum of 5 lung nodules, all ≤ 1.0 cm, and mesenteric or portal lymph nodes, all ≤ 2.0 cm), no curative treatment options, a Child–Pugh score of B7 or less, an Eastern Cooperative Oncology Group (ECOG) performance status of 0 or 1, no prior radioembolization, and no main-branch portal vein thrombosis.

Study Procedures

All patients were discussed by a multidisciplinary oncology board. Screening consisted of laboratory and physical examination, contrast-enhanced liver CT, liver MRI, hepatobiliary scintigraphy, and endoscopy of the upper gastrointestinal tract.

Patients received ondansetron, 8 mg, and dexamethasone, 10 mg, intravenously 1 h before angiography. Ursodeoxycholic acid, 300 mg twice daily, was given for 2 mo; prednisolone was given at a dose of 10 mg daily for the first month and 5 mg daily for the subsequent month (2 mo total), to reduce the chance of radioembolization-induced liver disease; and pantoprazole, 40 mg daily, was given for 6 wk (10).

A sheath was placed in the common femoral or radial artery, and a microcatheter was placed in the tumor-feeding artery or arteries. C-arm CT was performed at each intended target position. Then, a scout dose of ^{166}Ho -microspheres was administered for treatment simulation (QuiremScout, 250 MBq, ~ 3 million microspheres). The sheath stayed in situ during SPECT/CT imaging. Patients received treatment via a microcatheter at exactly the same position during a second angiography the same day.

The intended average absorbed dose in the perfused volume was 60 Gy: A (MBq) = $3.781 \times W$ (g), where A is the prescribed activity in megabecquerels and W is the target liver mass in grams (1 mL = 1.04 g) (7,8). Approximately 24 h after treatment, MRI was performed and the patients were discharged. Three to 5 d after treatment, the patients came back for posttreatment SPECT/CT. This scan was delayed to prevent detector dead time caused by the abundance of γ -photons (5).

Posttreatment follow-up at 3 and 6 wk and at 3 and 6 mo included blood and physical examinations, questionnaires, hepatobiliary scintigraphy (at 3 mo), and MRI (at 3 and 6 mo) (Supplemental Table 1; supplemental materials are available at <http://jnm.snmjournals.org>). Adverse events were assessed according to the Common Terminology Criteria for Adverse Events (CTCAE), version 4.03. Furthermore, during screening, shortly after treatment, and during follow-up, the core 30 and HCC 18-question module quality-of-life questionnaires of the European Organization for Research and Treatment of Cancer were used, as well as the brief pain inventory (short form).

Two independent radiologists who were not involved in the study proceedings performed masked random response assessment. In cases of discordance, a third radiologist was consulted to determine the final response category.

Quarterly interim safety analyses were presented to an independent data safety monitoring board.

Endpoints

The primary endpoint was the rate of unacceptable toxicity using CTCAE methodology, which was defined as grade 3 hyperbilirubinemia in combination with ascites and low albumin in the absence of disease progression (i.e., radioembolization-induced liver disease) or any serious adverse event or serious device defect possibly, probably, or causally related to treatment. Secondary endpoints included treatment efficacy, liver function, and quality of life. Dosimetric evaluation of pre- and posttreatment imaging fell outside the scope of this study.

Statistical Analysis

As a null hypothesis, it was assumed that the probability of unacceptable toxicity was 10% and that the alternative was a probability of

unacceptable toxicity of 25%. Unacceptable toxicity of 10% or less was considered acceptable and 25% or more was not. Consequently, a sample size of 30 patients was deemed appropriate. Statistical power (85%) quantified the probability of stopping the study early if toxicity was unacceptably high (type II error, 15%), which was arguably equally as important as wrongly stopping the study in the absence of true high toxicity (type I error, 15%), in line with previous reports (7,8).

The results shown are based on the per-protocol set, comprising patients who received both scout and therapeutic ^{166}Ho -microspheres. Overall survival was calculated from the date of treatment until the date of death by any cause or the end of registration (January 1, 2022). Kaplan–Meier curves and log-rank tests were used to evaluate overall survival. Responders (complete or partial response) and nonresponders (progressive or stable disease) were compared using landmark analysis with first and second response assessment. Variables with a 2-sided P value of less than 0.05 were deemed significant. Statistical analyses were performed using RStudio, version 1.2.5019.

RESULTS

From December 15, 2017, until January 22, 2020, 41 patients were included in the study. Eight patients failed screening because of main-branch portal vein thrombosis ($n = 2$), rapid tumor progression ($n = 2$), alternative treatment ($n = 1$), dismal liver function ($n = 1$), low glomerular filtration rate ($n = 1$), or worsened ECOG performance status ($n = 1$). Two additional patients discontinued the study because of a significant lung shunt or because they chose an alternative treatment. In total, 31 patients were treated with a scout and therapeutic dose of ^{166}Ho -microspheres (Fig. 1).

Baseline patient characteristics are given in Table 1. No cases with cavernous transformation were present. One patient previously underwent hemihepatectomy (right) followed by radiofrequency ablation of segments 2 and 3. One patient underwent resection of segments 6 and 7 and then underwent hemihepatectomy (right) followed by microwave ablation of segment 4, transarterial chemoembolization,

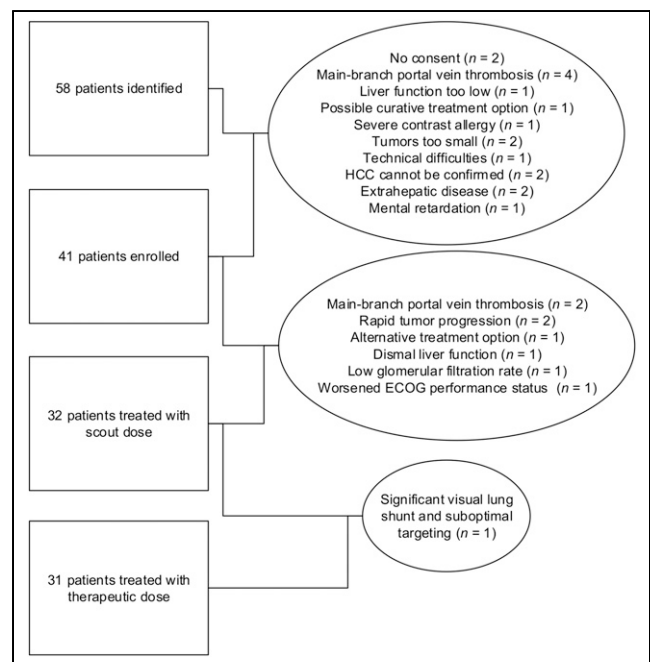


FIGURE 1. Flow diagram showing initial number of patients and those excluded for any given reason.

TABLE 1

Baseline Characteristics of HEPAR Primary Patients (n = 31)

Characteristic	Data	% or range
Sex		
Female	3	10
Male	28	90
Age (y)	73	44–85
Cirrhosis on imaging	20	65
Underlying liver disease*		
Alcohol abuse	20	65
Hepatitis B	1	3
Hepatitis C	4	13
Nonalcoholic fatty liver disease	3	10
Hemochromatosis	2	4
None of above	6	20
BCLC		
B	22	71
C	9	29
Bilirubin (μmol/L)	12	4–29
Albumin (g/L)	38.5	31–41.9
International normalized ratio	1.22	0.94–1.94
Thrombocytes (×10 ⁹ /L)	132	75–464
Child–Pugh score		
A5	19	61
A6	9	29
B7	3	10
Model-for-end-stage-liver-disease score	9	6–16
ECOG performance status		
0	18	58
1	13	42
Extrahepatic lesions		
None	27	87
Adrenal glands	4	13
Portal hypertension		
Thrombocytes < 150	18	58
Varices		
Small	9	29
Large	2	6
Imaging	14	45
Portal vein thrombosis		
Tumor thrombus	4	13
Nontumor thrombus	1	3
Mixed type	1	3
Bilobar disease†	17	55
Number of tumors		
1	4	13
2–3	4	13
>3	23	74
Tumor burden (%)	9.3	0.5–46.8
Largest tumor diameter (mm)	56	15 [‡] –195
Previous treatment*		
None	26	84
Resection	4	13
Ablation	4	13
Transarterial chemoembolization	1	1

*Some patients had more than 1 underlying liver problem.

†Only Liver Imaging Reporting and Data System 5 (definitely HCC) lesions were considered.

‡Patient had more than 15 small lesions.

*Some patients had more than 1 previous treatment.

Qualitative data are number and percentage; continuous data are median and range.

and wedge resection of segment 2. One patient underwent resection of segments 5 and 6 and microwave ablation of segment 4a. One patient underwent resection of segments 4b and 5. Finally, 1 patient previously underwent radiofrequency ablation of segments 6 and 7.

Treatment characteristics are summarized in Table 2. Unilobar treatment was performed in 20 of 31 (64%) patients, bilobar treatment (i.e., with at least 1 segment preserved) in 9 of 31 (29%), and whole-liver treatments in 2 of 31 (6%). Seven patients received a dose adjustment (median, –45%; range, –24%–56%) because of low hepatic function based on hepatobiliary scintigraphy (n = 4) or a per-procedural deviation from the planned treatment strategy (n = 3). The median absorbed dose to the target volume was 56 Gy (range, 27–90 Gy), and 23 patients received their intended dose. Twenty-eight patients received 1-d treatment. Three patients were treated at an interval of 7 d (n = 1), 35 d (reversible renal dysfunction, n = 1), or 168 d (malfunctioning aortic valve necessitating transarterial valve insertion first, n = 1). Median treatment efficiency (prescribed vs. net administered activity) was 95% (range, 74%–100%). On the basis of SPECT/CT imaging, the median anticipated lung dose resulting from shunting was 1 Gy (range, 0–16 Gy).

According to CTCAE, 120 laboratory-value adverse events were recorded, with no grade 4–5 events (Table 3). Furthermore, 168 clinical adverse events were observed, ranging from grades 1 to 5 (Table 4; Supplemental Tables 2 and 3). Most patients experienced a grade 1 or 2 increase in liver enzymes, with a maximum aspartate transaminase increase of grade 3 in 5 of 31 (16%) patients. However, the dynamic trajectory of these changes during 6 mo of follow-up did not show a clear peak or slope. Other than the expected lymphopenia, grade 2 or higher hematologic toxicity rarely occurred. Patients with type II diabetes mellitus (n = 14) experienced a high number of hyperglycemic adverse events, probably because of medication after treatment (i.e., steroids). Sixteen patients experienced grade 1 and 1 patient grade 2 back pain on the day of treatment, as they had to hold a supine position while undergoing a 1-d procedure.

Nineteen serious adverse events occurred, of which 4 events in 3 patients were related to treatment (3 possibly related and 1 definitely related). Two of these treatment-related events were from spontaneous bacterial peritonitis (both originated approximately 12 wk after treatment). One patient died of the infection after 1 d (treated with intravenous antibiotics), and the other patient recovered after 5 d (treated with intravenous and oral antibiotics). The third patient, with BCLC stage B, multifocal HCC, an ECOG performance status of 0, and previous treatment with resection and microwave ablation, experienced radiation-induced cholecystitis and cholangitis 1 mo after treatment, which developed into a biliary fistula (grade 3 bilirubin increase) and finally stabilized after endoscopic intervention. His liver function and clinical performance gradually declined until his death 1 y after treatment. Unrelated serious adverse events occurred more often in BCLC stage C patients (5/9 [56%]) than in BCLC stage B patients (4/22 [18%], P = 0.036). The treatment approach (i.e., uni- vs. bilobar) or previous liver-directed surgery could not be identified as a predictor of toxicity.

The median model-for-end-stage-liver-disease score was 9 (range, 6–16) at baseline and worsened to 10 (range, 7–20) at 6 mo after treatment. During 6 mo of follow-up, Child–Pugh scores fluctuated (Fig. 2). The 3 patients who experienced worsening of Child–Pugh score by 3 or 4 points (besides the patient with biliary fistula) had proven progression of disease. These patients received unilobar treatments and showed no signs of radioembolization-induced liver

TABLE 2
Procedure Characteristics (n = 31)

Characteristic	Data	% or range
Liver volume (mL)	1,941	1,036–3,460
Treated fraction (%)	54	16–100
Anticipated perfused volume average absorbed dose		
Per protocol (60 Gy)	24	77
Dose adjustments	7	23
Actual perfused volume average absorbed dose (Gy)	50	23–69
Treatment approach; all in 1 session		
Unilobar	20	64
Bilobar (excluding some segments)	9	29
Whole liver	2	6
Number of injection positions		
1	15	48
2	16	52
Interval scout therapy (d)	0	0–168
Prescribed activity (MBq)	3,998	1,080–11,451
Net administered activity (MBq)	3,717	1,001–10,420
Treatment efficiency (%)	95	74–100
Lung shunt on SPECT/CT (Gy)	1	0–16

Qualitative data are number and percentage; continuous data are median and range.

TABLE 3
Laboratory Adverse Events According to CTCAE, Version 4.03

Adverse event	Grade 1	Grade 2	Grade 3
AST increased	22/31 (71%)	2/31 (6%)	5/31 (16%)
Platelet count decreased	22/31 (71%)	1/31 (3%)	
INR increased	22/31 (71%)	2/31 (6%)	
AP increased	19/31 (61%)	5/31 (16%)	
Anemia	16/31 (52%)	5/31 (16%)	2/31 (6%)
ALT increased	15/31 (48%)	2/31 (6%)	
Hypoalbuminemia	14/31 (45%)	5/31 (16%)	1/31 (3%)
Prolonged APTT	13/31 (42%)	2/31 (6%)	
Hyponatremia	12/31 (39%)		3/31 (10%)
Hypokalemia	9/31 (29%)		
Hyperglycemia	9/31 (29%)	13/31 (42%)	6/31 (19%)
Creatinine increased	7/31 (23%)	1/31 (3%)	
Bilirubin increased	6/31 (19%)	4/31 (13%)	1/31 (3%)
GGT increased	5/31 (16%)	9/31 (29%)	14/31 (45%)
Hypoglycemia	3/31 (10%)		
Lymphopenia	1/31 (3%)	13/31 (42%)	9/31 (29%)

AST = aspartate transaminase; INR = international normalized ratio; AP = alkaline phosphatase; ALT = alanine transaminase; APTT = activated prothrombin time; GGT = γ -glutamyltransferase.

This table represents new and highest toxicity during 6-mo follow-up. No laboratory adverse events grade 4 or 5 were observed.

TABLE 4
Clinical Adverse Events Occurring in More Than 10% Patients or Grade 3–5 According to CTCAE, Version 4.03

Adverse event	Grade 1	Grade 2	Grade 3	Grade 4	Grade 5
Back pain	16/31 (52%)	1/31 (3%)			
Fatigue	13/31 (42%)	4/31 (13%)			
Ascites	7/31 (23%)	2/31 (6%)	1/31 (3%)		
Dyspnea	7/31 (23%)				
Nausea	6/31 (19%)	1/31 (3%)			
Abdominal pain	4/31 (13%)	2/31 (6%)	1/31 (3%)		
Dizziness	4/31 (13%)				
Edema limbs	4/31 (13%)	1/31 (3%)			
Fever	4/31 (13%)				
Hepatic pain	4/31 (13%)				
Itch	3/31 (10%)	1/31 (3%)			
Abdominal infection			1/31 (3%)		
Allergic reaction			1/31 (3%)		
Arthritis			1/31 (3%)		
Atrial fibrillation			1/31 (3%)		
Bile duct stenosis			1/31 (3%)		
Biliary fistula			1/31 (3%)		
Cholecystitis			1/31 (3%)		
Endocarditis infective				1/31 (3%)	
Esophageal varices hemorrhage			2/31 (6%)		
Gastric hemorrhage			1/31 (3%)		
Hepatic failure					2/31 (6%)
Hip fracture			1/31 (3%)		
Intracranial hemorrhage					1/31 (3%)
Ischemia cerebrovascular					1/31 (3%)
Lung infection			1/31 (3%)		
Sepsis			1/31 (3%)		

This table represents new and highest toxicity during 6-mo follow-up.

disease during the first 3 mo after treatment. Two other patients died of progressive disease and hepatic failure within 6 mo (considered unlikely to be related to treatment). Stratification per Child–Pugh score or ECOG performance status did not show any significant differences.

Twenty-six patients were evaluable according to mRECIST at 3 mo (2 died, 3 had insufficient imaging quality), and 19 patients were evaluable at 6 mo (2 more died, 3 left the study because of disease progression, 2 were lost to follow-up).

Independent review of the target liver lesions on MRI at 3 mo after treatment found, according to mRECIST, that 19% had a complete response, 35% a partial response, 42% stable disease, and 4% progressive disease (Figs. 3 and 4). A variable response specifically by the tumor thrombus in the portal vein was observed in 5 patients: 1 complete response, 1 partial response, 2 stable disease, and 1 lost to follow-up.

Five patients started sorafenib treatment, and 4 patients received immunotherapy after study treatment. Median overall survival was 14.9 mo (95% CI, 10.4–24.9 mo) (Fig. 5). The median post-landmark analysis overall survival of patients with either a complete or partial response of the total body according to mRECIST

at 3 mo was 16.6 mo (95% CI, 8.72 mo–not reached); it was 13 mo for nonresponders (95% CI, 8.95 mo–not reached, $P = 0.48$). The median overall survival of responders based on target liver lesions was not reached; for nonresponders, it was 12.8 mo (95% CI, 4.72–not reached, $P = 0.046$) (Supplemental Fig. 1).

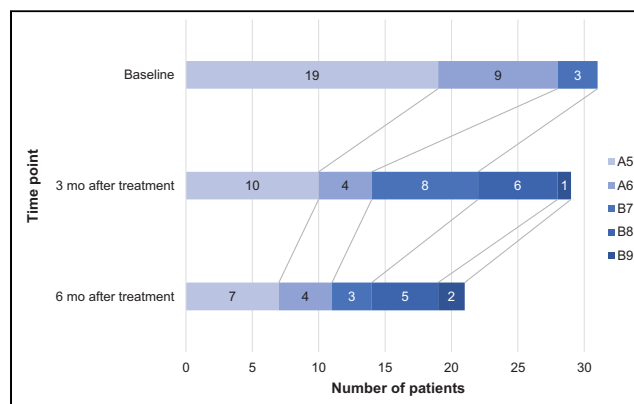


FIGURE 2. Child–Pugh score development over time.

The median α -fetoprotein level was 20 $\mu\text{g/L}$ (range, 2.0–240,000 $\mu\text{g/L}$) at baseline, with a median nadir of 6.6 $\mu\text{g/L}$ (range, 2.0–120,000 $\mu\text{g/L}$; 67% decrease). At baseline, median liver function based on hepatobiliary scintigraphy was 5.3%/min/m² (range, 2.0%–8.7%/min/m²), and 3 mo after treatment it was 4.4%/min/m² (range, 1.8%–9.2%/min/m²) ($P = 0.36$).

No clinically relevant change in quality of life (Supplemental Fig. 2) or pain (Supplemental Fig. 3) was observed.

DISCUSSION

This first (to our knowledge) prospective study on ¹⁶⁶Ho-microsphere radioembolization in HCC confirmed safety. During and after ¹⁶⁶Ho-microsphere radioembolization, quality of life was maintained, and pain and toxicity were mild and manageable. Furthermore, a pronounced antitumor effect was found.

A low-activity scout dose of ¹⁶⁶Ho-microspheres—limited enough not to cause tissue damage—can be used instead of the commonly used scout dose of ^{99m}Tc-macroaggregated albumin particles (^{99m}Tc-MAA) (11). In contrast to ^{99m}Tc-MAA, the scout dose of ¹⁶⁶Ho-microspheres is not administered as a bolus injection, but slowly. The extrahepatic (i.e., lung shunting) and intrahepatic dose distribution can be predicted more accurately than for ^{99m}Tc-MAA (12,13). A scout dose of ¹⁶⁶Ho-microspheres was superior, with a median score of 4, versus 2.5 for ^{99m}Tc-MAA ($P < 0.001$; visually assessed from 1 to 5), which was confirmed in a quantitative

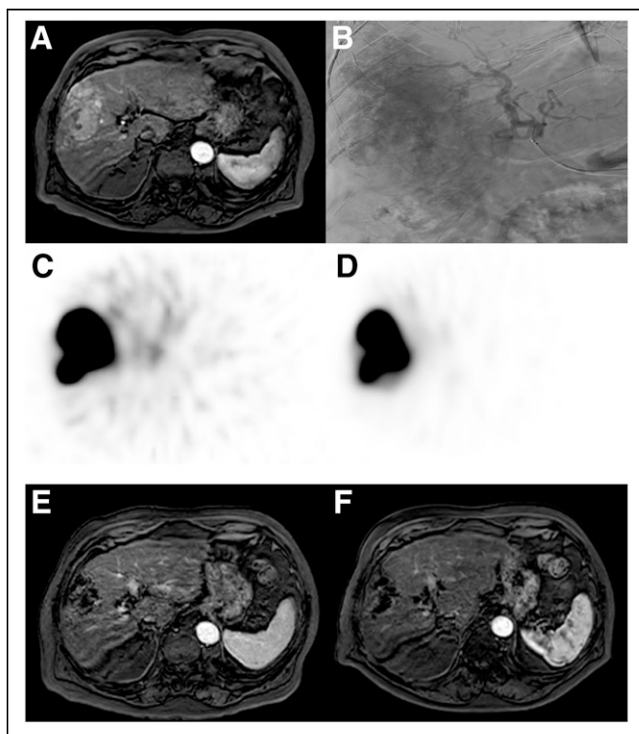


FIGURE 3. An 85-y-old patient with HCC, no underlying liver disease, and no previous treatment (ECOG performance status 1, Child–Pugh score A5, BCLC stage B) with large hypervascular tumor spanning segments 4–8 (A, axial contrast-enhanced MRI) that had multiple tumor-feeding vessels from right hepatic artery (B, digital subtraction angiography). He received ¹⁶⁶Ho-microsphere scout procedure and SPECT (C), which showed good targeting of tumor. Scout procedure proved highly predictive for posttreatment ¹⁶⁶Ho-microsphere distribution (D) and resulted in complete response of target liver lesions at 3 mo (E, axial contrast-enhanced MRI) and 6 mo (F, axial contrast-enhanced MRI).

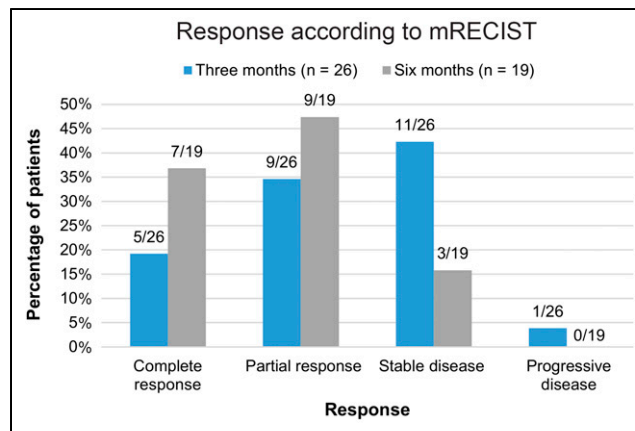


FIGURE 4. Response assessment of target liver lesions at 3 and 6 mo after treatment with ¹⁶⁶Ho-microsphere radioembolization according to mRECIST. Some patients did not undergo imaging at 3- or 6-mo follow-up because of death ($n = 2$ and 8, respectively) or withdrawn consent ($n = 2$ or 0, respectively). Some patients were not evaluable because of absence of arterial enhancement of tumor or low-quality imaging (e.g., artifacts or breathing motion) ($n = 3$ and 2, respectively).

analysis. In contrast, in the SARAH trial, in which ^{99m}Tc-MAA was used as a scout, only 52% “optimal agreement” between pretreatment ^{99m}Tc-MAA distribution and posttreatment resin ⁹⁰Y-microsphere distribution was found (14).

The specific activity of ¹⁶⁶Ho-microspheres (i.e., ± 340 Bq/sphere) is higher than that of resin ⁹⁰Y-microspheres (i.e., ± 50 Bq/sphere) and lower than that of glass ⁹⁰Y-microspheres (i.e., $\pm 1,250$ – $2,500$ Bq/sphere). At lower specific activities, a higher number of microspheres needs to be injected to reach the same absorbed dose. This is reflected in the relatively high incidence of adverse events related to the postembolization syndrome in the current study (e.g., pain [22%], nausea [22%], and fatigue [55%]). Moreover, differences in product characteristics will translate to different dose thresholds with regard to safety and efficacy, because of differences in dose distributions (15). For ¹⁶⁶Ho radioembolization in HCC, these dose thresholds need to be established for patient selection and treatment planning. In 36 patients with a total of 98 tumors of different metastatic origins, a significant difference was found between patients with complete or partial response (210 Gy; 95% CI, 161–274 Gy) and patients with progressive disease (116 Gy; 95% CI, 81–165 Gy) (16). Additionally, dose

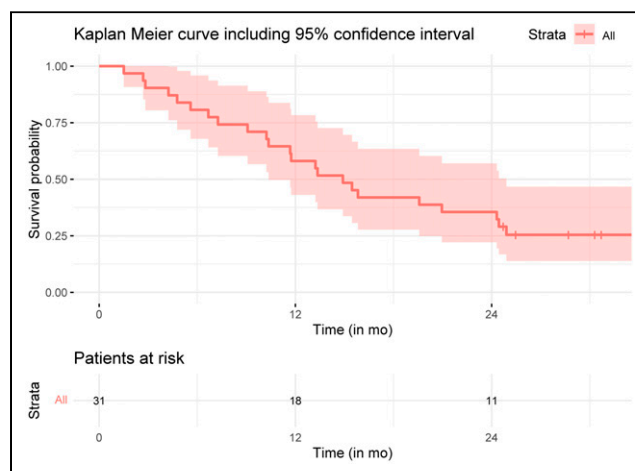


FIGURE 5. Overall survival of HEPAR Primary patients.

thresholds were confirmed in colorectal cancer, also looking at safety thresholds for nontumorous liver tissue. The median parenchyma-absorbed dose was 37 Gy (range, 12–55 Gy). The mean difference in parenchyma-absorbed dose for patients with CTCAE grade 0–2 versus CTCAE grade 3–5 was 12 Gy (95% CI, 3.4–19.7; $P = 0.0070$) (17). For HCC patients, however, separate dose thresholds will need to be established, including considerations with regard to treatment intent (i.e., palliative setting as in the current setting vs. potential curative settings: radiation segmentectomy and lobectomy) (18,19).

These dosimetric considerations should be balanced with baseline patient characteristics such as laboratory values, Child–Pugh status, performance score, and BCLC stage. Because of the relatively low number of patients in the current study, no definite conclusions could be drawn on patient selection. At the same time, differences in patient characteristics between studies also limit direct comparison. The SARAH, SIRveNIB, and SORAMIC randomized controlled trials on resin ^{90}Y -microsphere radioembolization (14,20–23), and the DOSISPHERE-01 study on glass ^{90}Y -microsphere radioembolization (24), included more advanced-stage C BCLC, limiting toxicity and efficacy comparison. Nevertheless, a 23% rate of adverse events grade 3 or higher, a median overall survival of 14.9 mo, and a 3-mo response rate of 54% in the present study seem favorable. In the SARAH, SIRveNIB, and SORAMIC trials, adverse events of grade 3 or higher were observed in 27%, 28%, and 25% of the patients, respectively. The best overall response rate in the SARAH trial was 19%, the reported best tumor response in the SIRveNIB trial was 23.1%, and tumor response was not analyzed in the SORAMIC trial. The objective response rate was 35.7% in the patients in the DOSISPHERE-01 study, whose treatment was based on a predefined average absorbed dose in the perfused volume, as was used in the present study.

One of the limitations of this study was the relatively limited number of patients and the heterogeneous patient and disease characteristics, besides the fact that the study had a noncomparative design. In the current study, radioembolization treatment planning was performed according to a standard approach, regardless of tumor and functional liver dosimetry (25). A single-day treatment approach is beneficial from a patient perspective with regard to number of hospital visits, preparation, and recovery (24,26). However, a single-day treatment strategy does not allow for dosimetry-based treatment planning since patient-specific treatment activity needs to be preordered. Another limitation was that the methods used for response evaluation (modified RECIST [mRECIST]) have inherent limitations (e.g., local vs. systemic evaluation, relation to overall survival), but contrast enhancement on MRI may also be hampered by holmium-induced artifacts, since ^{166}Ho -microspheres cause loss of signal on T1-weighted MRI scans and make it more difficult to measure viable tumor (6).

Concomitant use of different therapies in patients with HCC is of special interest, such as adjuvant immunotherapy after resection or ablation to decrease the chance of recurrence (27). But also of interest is the combination of immunotherapy with other local or regional treatment options, including transarterial chemoembolization and radioembolization (28,29). These combined approaches are expected to cause more toxicity, which may be seen as a clear call for more control. Radioembolization may offer that control by offering dosimetry-based individualized treatment planning. ^{166}Ho -microsphere radioembolization offers the unique combination of procedural control and individualized treatment by using a predictive scout dose of the exact same ^{166}Ho -microspheres and performing

treatment planning based on accurate dosimetry (12). However, dose thresholds for an effective tumor-absorbed dose and a safe functional liver-absorbed dose need to be established in larger series.

CONCLUSION

This interventional, nonrandomized study showed an acceptable low rate of ^{166}Ho radioembolization–related serious toxicity (3/31 patients; <10%) in patients with HCC. Furthermore, 54% of tumor lesions showed a response (mRECIST) at 3 mo after treatment. ^{166}Ho radioembolization may be considered a safe and effective alternative treatment option in selected patients with HCC of BCLC stage B or C.

DISCLOSURE

This study was financed mainly by a grant from the Dutch Cancer Society (KWF Kankerbestrijding, project 10307) and was financially supported by the Radiology and Nuclear Medicine Department of the University Medical Center Utrecht. Quirem Medical B.V. supplied the holmium microspheres free of charge. Margot Reinders acted as a speaker for Boston Scientific/BTG (personal fees) and was funded by the Dutch Cancer Society (KWF Kankerbestrijding) via a grant received by Marnix Lam. Karel van Erpecum was on the advisory board of AOP Orphan Pharmaceuticals AG in 2020 and is a member of HepNed and Hepatitis C Elimination in The Netherlands (CELINE—a cooperation between university medical centers in The Netherlands for elimination of hepatitis C viral infection from The Netherlands, sponsored by Gilead). Maarten Smits acted as a speaker for Boston Scientific/BTG (personal fees and nonfinancial support). Arthur Braat acted as a speaker for Boston Scientific/BTG (personal fees and nonfinancial support) and Terumo (nonfinancial support). Marnix Lam acted as a speaker for Boston Scientific/BTG (personal fees and nonfinancial support) and Terumo (nonfinancial support) and received a grant from the Dutch Cancer Society (KWF Kankerbestrijding). No other potential conflict of interest relevant to this article was reported.

ACKNOWLEDGMENTS

We thank the patients for participating in this study; the independent radiologists Manon N.G.J.A. Braat and Frank J. Wessels for reviewing all the patient images; the Department of Radiology and Nuclear Medicine of the University Medical Centre Utrecht for cofunding this study; Tjitske Kent-Bosma (clinical research coordinator, University Medical Centre Utrecht) for contributing to study coordination; and the gastroenterology departments of both the University Medical Centre Utrecht and Erasmus MC University Medical Centre Rotterdam for recruiting patients.

KEY POINTS

QUESTION: Is ^{166}Ho radioembolization a safe treatment option for patients with HCC?

PERTINENT FINDINGS: This interventional, nonrandomized study showed an acceptably low rate of ^{166}Ho radioembolization–related serious toxicity (3/31 patients; <10%) in patients with HCC. Furthermore, 54% of tumor lesions showed a response (mRECIST) at 3 mo after treatment.

IMPLICATIONS FOR PATIENT CARE: ^{166}Ho radioembolization may be considered a safe and effective alternative treatment option in selected patients with HCC of BCLC stage B or C.

REFERENCES

1. Sangiovanni A, Colombo M. Treatment of hepatocellular carcinoma: beyond international guidelines. *Liver Int.* 2016;36(suppl 1):124–129.
2. Finn RS, Qin S, Ikeda M, et al. Atezolizumab plus bevacizumab in unresectable hepatocellular carcinoma. *N Engl J Med.* 2020;382:1894–1905.
3. Johnston MP, Khakoo SI. Immunotherapy for hepatocellular carcinoma: current and future. *World J Gastroenterol.* 2019;25:2977–2989.
4. Kallini JR, Gabr A, Salem R, Lewandowski RJ. Transarterial radioembolization with yttrium-90 for the treatment of hepatocellular carcinoma. *Adv Ther.* 2016;33:699–714.
5. Elschot M, Nijssen JFW, Dam AJ, de Jong HWAM. Quantitative evaluation of scintillation camera imaging characteristics of isotopes used in liver radioembolization. *PLoS One.* 2011;6:e26174.
6. van de Maat GH, Seevinck PR, Elschot M, et al. MRI-based biodistribution assessment of holmium-166 poly(L-lactic acid) microspheres after radioembolisation. *Eur Radiol.* 2013;23:827–835.
7. Smits MLJ, Nijssen JFW, van den Bosch MAAJ, et al. Holmium-166 radioembolisation in patients with unresectable, chemorefractory liver metastases (HEPAR trial): a phase 1, dose-escalation study. *Lancet Oncol.* 2012;13:1025–1034.
8. Prince JF, van den Bosch MAAJ, Nijssen JFW, et al. Efficacy of radioembolization with ¹⁶⁶Ho-microspheres in salvage patients with liver metastases: a phase 2 study. *J Nucl Med.* 2018;59:582–588.
9. Heimbach JK, Kulik LM, Finn RS, et al. AASLD guidelines for the treatment of hepatocellular carcinoma. *Hepatology.* 2018;67:358–380.
10. Gil-Alzugaray B, Chopitea A, Iñarrairaegui M, et al. Prognostic factors and prevention of radioembolization-induced liver disease. *Hepatology.* 2013;57:1078–1087.
11. Braat AJ, Prince JF, van Rooij R, Bruijnen RCG, van den Bosch M, Lam M. Safety analysis of holmium-166 microsphere scout dose imaging during radioembolisation work-up: a cohort study. *Eur Radiol.* 2018;28:920–928.
12. Smits MLJ, Dassen MG, Prince JF, et al. The superior predictive value of ¹⁶⁶Ho-scout compared with ^{99m}Tc-macroaggregated albumin prior to ¹⁶⁶Ho-microspheres radioembolization in patients with liver metastases. *Eur J Nucl Med Mol Imaging.* 2020;47:798–806.
13. Elschot M, Nijssen JFW, Lam MGEH, et al. ^{99m}Tc-MAA overestimates the absorbed dose to the lungs in radioembolization: a quantitative evaluation in patients treated with ¹⁶⁶Ho-microspheres. *Eur J Nucl Med Mol Imaging.* 2014;41:1965–1975.
14. Hermann AL, Dieudonné A, Ronot M, et al. Relationship of tumor radiation-absorbed dose to survival and response in hepatocellular carcinoma treated with transarterial radioembolization with ⁹⁰Y in the SARAH study. *Radiology.* 2020;296:673–684.
15. Pasciak AS, Abiola G, Liddell RP, et al. The number of microspheres in Y90 radioembolization directly affects normal tissue radiation exposure. *Eur J Nucl Med Mol Imaging.* 2020;47:816–827.
16. Bastiaannet R, van Roekel C, Smits MLJ, et al. First evidence for a dose-response relationship in patients treated with ¹⁶⁶Ho radioembolization: a prospective study. *J Nucl Med.* 2020;61:608–612.
17. van Roekel C, Bastiaannet R, Smits MLJ, et al. Dose-effect relationships of ¹⁶⁶Ho radioembolization in colorectal cancer. *J Nucl Med.* 2021;62:272–279.
18. Salem R, Padia SA, Lam M, et al. Clinical and dosimetric considerations for Y90: recommendations from an international multidisciplinary working group. *Eur J Nucl Med Mol Imaging.* 2019;46:1695–1704.
19. Levillain H, Bagni O, Deroose CM, et al. International recommendations for personalised selective internal radiation therapy of primary and metastatic liver diseases with yttrium-90 resin microspheres. *Eur J Nucl Med Mol Imaging.* 2021;48:1570–1584.
20. Vilgrain V, Pereira H, Assenat E, et al. Efficacy and safety of selective internal radiotherapy with yttrium-90 resin microspheres compared with sorafenib in locally advanced and inoperable hepatocellular carcinoma (SARAH): an open-label randomised controlled phase 3 trial. *Lancet Oncol.* 2017;18:1624–1636.
21. Chow PKH, Gandhi M, Tan SB, et al. SIRveNIB: selective internal radiation therapy versus sorafenib in Asia-Pacific patients with hepatocellular carcinoma. *J Clin Oncol.* 2018;36:1913–1921.
22. Ricke J, Bulla K, Kolligs F, et al. Safety and toxicity of radioembolization plus sorafenib in advanced hepatocellular carcinoma: analysis of the European multicentre trial SORAMIC. *Liver Int.* 2015;35:620–626.
23. Ricke J, Klumpen HJ, Amthauer H, et al. Impact of combined selective internal radiation therapy and sorafenib on survival in advanced hepatocellular carcinoma. *J Hepatol.* 2019;71:1164–1174.
24. Garin E, Tselikas L, Guiu B, et al. Personalised versus standard dosimetry approach of selective internal radiation therapy in patients with locally advanced hepatocellular carcinoma (DOSISPHERE-01): a randomised, multicentre, open-label phase 2 trial. *Lancet Gastroenterol Hepatol.* 2021;6:17–29.
25. Bastiaannet R, Kappadath SC, Kunnen B, Braat A, Lam M, de Jong H. The physics of radioembolization. *EJNMMI Phys.* 2018;5:22.
26. van Roekel C, Harlianto NI, Braat A, et al. Evaluation of the safety and feasibility of same-day holmium-166: radioembolization simulation and treatment of hepatic metastases. *J Vasc Interv Radiol.* 2020;31:1593–1599.
27. Hack SP, Spahn J, Chen M, et al. IMbrave 050: a phase III trial of atezolizumab plus bevacizumab in high-risk hepatocellular carcinoma after curative resection or ablation. *Future Oncol.* 2020;16:975–989.
28. Makary MS, Khandpur U, Cloyd JM, Mumtaz K, Dowell JD. Locoregional therapy approaches for hepatocellular carcinoma: recent advances and management strategies. *Cancers (Basel).* 2020;12:1914.
29. Waidmann O. Recent developments with immunotherapy for hepatocellular carcinoma. *Expert Opin Biol Ther.* 2018;18:905–910.